Modulation of Kinesin Half-Site ADP Release and Kinetic Processivity by a Spacer between the Head Groups†

David D. Hackney,* Maryanne F. Stock, Jodi Moore, and Reid A. Patterson

Department of Biological Sciences, Carnegie Mellon University, 4400 Fifth Avenue, Pittsburgh, Pennsylvania 15213

Received May 29, 2003; Revised Manuscript Received August 1, 2003

ABSTRACT: A series of modifications of the junction of the neck linker and neck coil of dimeric *Drosophila* kinesin were constructed to determine the influence of head orientation and spacing on the ATPase kinetics. Ala^{345} is the first residue in the coiled-coil of the neck, and its replacement with glycine or proline produces no significant change in the k_{cat} or $K_{0.5(MT)}$ values for activation of their ATPase by microtubules (MTs) or in their $k_{bi(ratio)}$ value for the average number of ATP molecules hydrolyzed during a processive encounter with a MT. Addition or deletion of a single amino acid at the junction produces only modest changes with less than a 2-fold reduction in kinetic processivity. Insertion of a spacer of 6 or 12 additional amino acids at the neck linker junction increases the $K_{0.5(MT)}$ value by 3−4-fold with a corresponding decrease in kinetic processivity. The sliding velocities of all the mutant constructs under multimotor conditions are within 30% of the wild-type value. All the constructs with single residue changes exhibit half-site ADP release on binding to MTs. The constructs with long insertion, however, rapidly release both ADP molecules per dimer on binding to a MT, indicating that the steric constraints that prevent release of ADP from the tethered head of wild-type kinesin have been relieved by the long insertions. The constructs with long inserts have decreased kinetic processivity and dissociate from the MT during ATP hydrolysis 3-fold faster than wild-type.

Kinesin is a motor protein that moves along MTs,[1] coupled to ATP hydrolysis (*1*−*3*). A striking feature of kinesin motility is that it is highly processive (*4*, *5*). A single kinesin dimer is able to move along a MT at ∼600 nm/s for distances of ∼1 μm before dissociation. Kinesin moves in steps of 8 nm (equal to the spacing of tubulin heterodimers along a protofilament), and each step is likely coupled to hydrolysis of one ATP molecule. Run lengths of 1 μm would thus require hydrolysis of ∼100 ATP molecules per dimer during each productive encounter with a MT. Studies of the ATPase properties of kinesin and MTs in solution are consistent with such motility (see ref *6*). The k_{cat} value of ∼80 s^{-1} per dimer and a step size of 8 nm per ATP predict a sliding velocity of 640 nm s^{-1} that is consistent with the observed velocity of sliding at the single molecule level. The $k_{bi(ratio)}$ values, for the average number of ATP molecules hydrolyzed per encounter with a MT, are equal to the number of 8-nm steps observed in the processive runs.

Hydrolysis of ATP and release of Pi by kinesin are fast, and the rate-limiting step in the absence of MTs is the slow release of ADP (*7*). Binding of the kinesin·ADP complex to MTs accelerates ADP release and results in a tight MT·kinesin complex in the absence of nucleotides. Addition of dimeric kinesin motor domain (head) constructs to MTs results in release of only half of the bound ADP with formation of a tethered intermediate (species II in Scheme 1). This tethered intermediate has one head attached tightly to the MT without bound ADP, and the other head retains its ADP (*8*) but is still tethered to the MT by the tightly attached head. The ADP bound to the tethered head is, however, rapidly released when ATP binds to the attached head. This coupling of the ATPase cycles of the two heads provides an attractive explanation for how the dimer can maintain attachment to the MT through many ATPase cycles, while the individual heads must be continually detaching from one MT site so that they can reattach to a new site further toward the plus end of the MT.

At the structural level, the most likely explanation for why the tethered head cannot rapidly release ADP is that the steric constraints of the linkage between the two head domains prevent the tethered head from being able to "reach" to a neighboring MT binding site while the other head is rigidly attached (see Figures 1 and 2). Even if the tethered head is able to form a weak binding interaction with a MT binding site, it does not have the steric freedom to adopt a conformation that leads to rapid ADP release. In the nomenclature of Rice et al. (*9*), the dimer is held together by the coiled-coil of the neck coil and is linked to the core of the motor domain by the neck linker, which is docked against the motor core and in an extended conformation, as shown in Figure 1B. For a wild-type dimer to bind to the MT with both head domains, either the neck linkers must undock and allow the heads to move independently, or the coiled-coil of the neck coil must unwind (or a combination). Rice et al. (*9*) have provided evidence that the neck coil is largely disordered in the absence of a bound nucleotide or with ADP but becomes docked when attached to the MT

† Supported by Grant NS28562 from the National Institutes of Health.

* To whom correspondence should be addressed. Tel.: (412) 268-3244. Fax: (214) 268-7129. E-mail: ddh+@andrew.cmu.edu.

[1] Abbreviations: mantADP, 2′(3′)-*O*-(*N*-methylantraniloyl)adenosine 5′-diphosphate; MT, microtubule.

10.1021/bi0349118 CCC: $25.00
Published on Web 09/18/2003

Scheme 1: Scheme for MT-ATPase of Dimeric Kinesin[a]

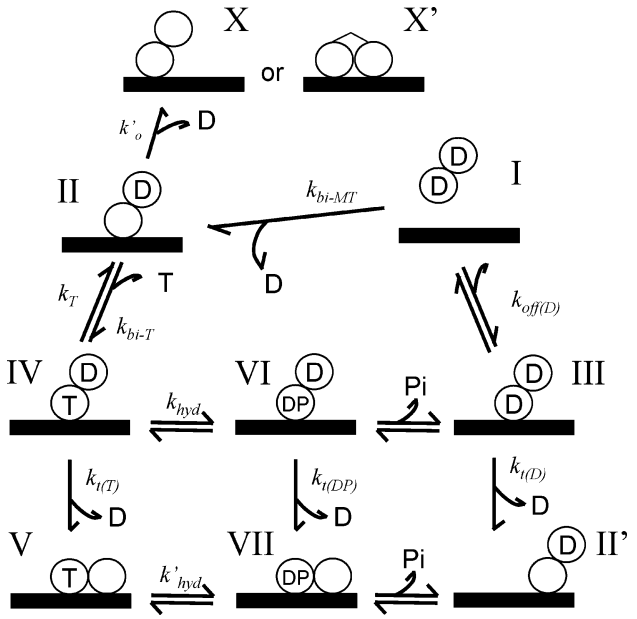

[a] Adapted from ref *15*. The paired circles represent the DKH405 dimer, and the solid bar represents a MT. ADP, ADP, and Pi are indicated by D, T, and P, respectively. In this model, $k_{bi(ADP)}$ for the bimolecular rate of ADP release in the presence of excess ATP is approximately equal to k_{bi-MT} because both ADP molecules per dimer are released in rapid succession in the presence of ATP.

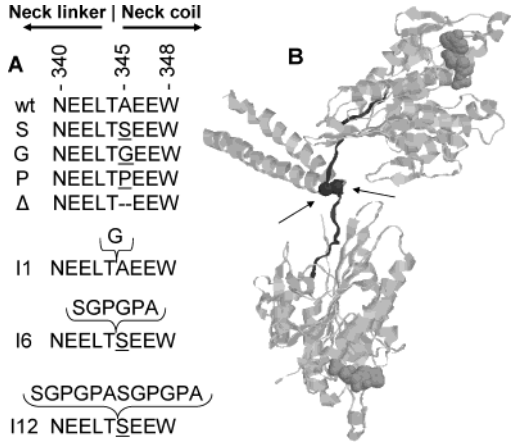

FIGURE 1: Junction mutants. (A) Sequences for the mutations introduced at the junction of the neck linker and the neck coil. The wild-type sequence for positions 340−348 of *Drosophila* kinesin is included for comparison. Amino acid changes at the position in the mutants corresponding to Ala[345] are underlined. Because the properties of the G and P substitutions are similar to those of wild-type, the more conservative S substitution was not investigated in detail. (B) Location of Ala[345] at the first position of the neck coil. View was generated by Rasmol (*37*) from the coordinates for the rat kinesin dimer (*20*). Ala[345] of *Drosophila* kinesin is homologous to Ala[339] of rat kinesin, and the α carbon atoms of this residue in both chains are indicated in black spacefill (arrows). The rest of the protein is given as a ribbon diagram, with the neck linker shown in a darker shade. The ADP molecule in each head is indicated in spacefill.

with a bound ATP analogue. ATP-induced docking of the neck linker might facilitate dissociation of the trailing head and movement toward the lead position to allow the tethered head to interact productively with the MT and release ADP. However, a freely mobile neck linker should also allow the tethered head to productively reach the next site with release of ADP, and the structural basis for the inhibition of ADP

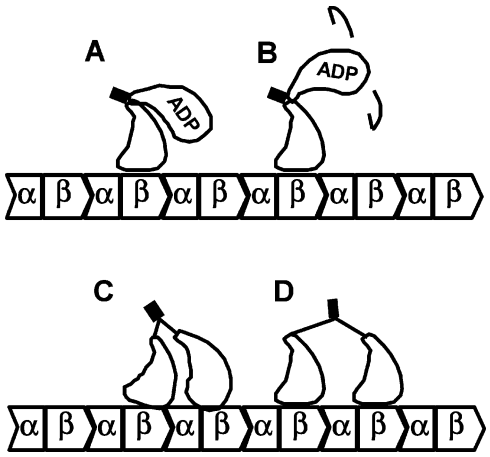

FIGURE 2: Models for the tethered complex of junction mutant constructs. The neck coil is indicated by a solid rectangle. The detailed conformation of the tethered intermediate for wild-type kinesin (A) is not established and may be variable. The schematic drawings of the tethered intermediate in this figure and in Scheme 1 are not meant to imply a particular favored geometry. It is also possible that the wild-type tethered head can form a weak binding interaction with an adjacent tubulin binding site without being able to achieve the conformation necessary to induce rapid ADP release. In B, changes in the junction have introduced increased disorder and altered orientation, without increasing the length. In C and D, introduction of a spacer at the junction allows the tethered head to productively interact with the MT and results in release of ADP, with C being strained and D unstrained.

release from the tethered head is not known. One possibility is that the undocked neck linker is not freely mobile and is restrained to conformations that so not allow ADP release. Regardless of the detailed structural mechanism, though, some conformational restraint in the dimer−MT complex prevents both heads from releasing ADP, and the insertion of a spacer between the heads might allow both heads to productively interact with the MT and accelerate the release of ADP from the tethered head. We report here that changes to the junction of the neck coil and neck linker that can introduce disorder or length changes of plus or minus one residue have only modest effects on kinetic processivity, whereas insertions of 6 or 12 residues markedly accelerate the release of ADP from the tethered head in the absence of nucleotide binding to the attached head.

MATERIALS AND METHODS

Mutant Construction and Expression. The S, G, P, Δ, and I1 mutations, as described in Figure 1, were generated by PCR. The wild-type sequence of ACTGCCGAG for amino acid resides T344, A345, and E346 (*10*) was replaced with ACTAGTGAG, ACTGGGGAG, ACTCCCGAG, ACT-GAG, and ACTGGGGCCGAG, respectively. pDKH405-S also contains a new *Spe*I site (underlined). These PCR products were introduced into wild-type pDKH405 (*11*) such that only the region from the *Pst*I site at amino acid position 295 to the C-terminal is PCR-derived. One or two copies of the phosphorylated self-complementary oligonucleotide CTAGCGGGCCCGGGCCCG with *Spe*I-compatible over-hangs were introduced into the *Spe*I site of pDKH405-S to produce DKH405-I6 and DKH405-I12, respectively. These mutant constructs in the DKH405 background were sequentially subcloned into DKH559-RC using the BssH1 site at amino position 374 and then into DKH960 (*12*) using the

AlwN1 site at amino acid position 448. DKH559-RC is *Drosophila* kinesin from position 1 to 559, with the sequence GGGRKCH appended to the C-terminal. This introduces a highly reactive cysteine residue (*13*).

The PCR-derived regions of the final DKH960 constructs were confirmed by DNA sequencing for all mutants except I12. This construct has an extended palindromic repeat with high GC content, and the sequencing DNA polymerase was not able to read completely through this region, even with modifications designed for high GC templates. To determine the number of copies of the cassette that were inserted into DKH405-I12, MALDI/TOF mass spectrometry analysis was performed. The parent ions of both wild-typeDKH405 and DKH405-I12 were overlapping doublets with *m*/*z* values for the singly charged species of 45 254 and 45 446 for DKH405 and 46 218 and 46 394 for DKH405-I12, using apomyoglobin for calibration. The change in *m*/*z* between the species at higher *m*/*z* for DKH405 and DKH405-I12 is 948, which agrees with the predicted difference of 949 for two copies of the cassette. These values are in reasonable agreement with the predicted values of 45 376 and 46 324 for unprocessed wild-type and I12 peptides that still contain Met^1. The differences in the absolute values are likely due to the calibration, as a separate determination with wild-type DKH405 gave 45 374 for the peak at higher *m*/*z* when calibrated against bovine serum albumin.

The DKH405 mutant proteins were expressed in *Escherichia coli* and purified by chromatography on phosphocellulose and DEAE-Biogel essentially as described previously (*11*, *14*). Mutant DKH960 proteins for use in motility assays were purified by chromatography on phosphocellulose and ammonium sulfate precipitation only (*12*, *14*). DKH405-I1, DKH405-I6, and DKH405-I12 eluted similarly to wild-type DKH405 on gel filtration chromatography (*11*), indicating that the mutant constructs are also dimeric. MTs were prepared as previously described (*15*). Most of the experiments were preformed on MTs prepared with bovine tubulin, but pig tubulin was also used as indicated. All concentrations of kinesin are given as the concentration of motor domains, and the concentration of MTs is expressed as the concentration of tubulin heterodimers.

Kinetic and Motility Measurements. All reactions were conducted at 25 °C in A25 buffer (*16*) supplemented with 25 mM KCl, except as indicated. ATPase assays were performed using the coupling system of pyruvate kinase and lactic dehydrogenase as described (*17*, *18*). Fluorescence measurements were obtained on an Applied Photophysics SX.18 instrument as described (*15*) with excitation at 356 nm. Measurements are reported as ±standard error, but in some cases they are reported as ±standard deviation (number of determinations) to emphasize the broad spread in the individual values.

Motility in the multimotor mode was determined essentially as described previously (*19*) by DIC microscopy using salt-washed sea urchin axonemes and mutant proteins that had been subcloned into DKH960. Briefly, a flow cell was washed sequentially with sufficient kinesin to saturate surface binding, 0.5 mg/mL casein, and then axonemes with 0.5 mg/mL casein and 1 mM MgATP. The motility buffer was A25 with 25 mM KCl, and observations were made at approximately 25 °C by adjustment of the room temperature.

RESULTS

Rationale for Design of Junction Mutations. The junction mutations indicated in Figure 1A were designed to provide a range of potential changes in the disruption of the coordination of the two heads of the kinesin dimer. The changes were introduced at Ala^{345}, which is indicated by arrows in Figure 1B. This is the first residue in the hydrophobic repeat of the predicted neck coil and is, in fact, observed to be the first residue in X-ray crystal structures in which the neck coil is ordered (*20*). Changes at this position should change the functional coupling of the neck linker and the neck coil, without grossly altering the conformation of either one, except for possible changes in the first heptad of the neck coil. Potential situations are illustrated schematically in Figure 2, with case A corresponding to the wild-type situation with a tethered intermediate that cannot reach the next tubulin binding site to allow release of the ADP on the tethered head. Substitution of Ala^{345} with Gly or Pro can potentially introduce disorder at the junction, or at least an alteration of the wild-type orientation of the heads with respect to each other and the neck coil, but without increase in the length of the linker. This situation is illustrated by case B with increased disorder, but with the tethered head still not able to reach far enough to bind productively with release of ADP. Changing the length of the junction region by deletions or insertions can also introduce disorder, but in addition will influence the ability of the tethered head to reach the next tubulin binding site with productive release of ADP. In case C, the tethered head can reach productively but is strained, and this would influence the rate of ADP release and the energetics of the steps. In the final case D, the spacer is long enough to allow both heads to interact productively without significant strain. The detailed conformation of dimer constructs bound to the MT is controversial (see ref *21*), and it is possible that the tethered intermediate of even wild-type dimers physically resembles case C or D, with both heads interacting with the MT but with one head still unable to adopt a conformation leading to rapid ADP release. Similar possibilities for a tethered intermediate have also been considered for myosin interacting with actin (*22*−*25*).

ATPase and Motility Properties. The basal rate of ADP release for all constructs in the absence of MTs was low, at $\leq 0.01\ s^{-1}$ (not shown), and thus similar to the wild-type value. The MT-stimulated ATPase and motility properties of the mutant junction constructs are summarized in Table 1. Substitution of Ala^{345} of DKH405 with P or G produces essentially no change in the ATPase properties, kinetic processivity, or sliding velocity. The constructs with a one-residue deletion (Δ) or insertions of 1, 6, or 12 residues (I1, I6, and I12, respectively) have a small decrease (≤20%) in k_{cat} at saturating MT levels with a decrease of similar magnitude in the sliding velocity. The principal effect is an increase in the $K_{0.5(MT)}$ value with a corresponding decrease in kinetic processivity as measured by (i) the $k_{bi(ratio)}$ value for the average number of ATP molecules hydrolyzed per productive encounter with a MT and (ii) the $k_{off(ATPase)}$ value for the rate of net dissociation of dimeric kinesin from the MT during steady-state ATP hydrolysis. The $k_{off(ATPase)}$ values were calculated with the assumption that $K_{0.5(MT)}$ equals the K_d for binding of the motor to the MTs during steady-state ATP hydrolysis, and this has been confirmed for wild-type

Table 1: ATPase and Motility of Junction Constructs

DKH405	k_{cat}[a] (s^{-1})	$K_{0.5(MT)}$[a] (μM)	$k_{bi(ADP)}$[b] (μM^{-1} s^{-1})	$k_{bi(ratio)}$[c] (s^{-1})	$k_{off(ATPase)}$[d] (μm s^{-1})	motility[e]
wt	43.3 ± 0.5	0.123 ± 0.006	5.73 ± 0.16	61.4	0.70	0.449 ± 0.051 (57)
G	43.6 ± 0.8	0.115 ± 0.010	6.09 ± 0.19	62.3	0.70	0.491 ± 0.085 (46)
P	41.2 ± 0.5	0.114 ± 0.006	6.68 ± 0.39	54.1	0.76	0.438 ± 0.051 (43)
Δ	36.6 ± 0.6	0.134 ±0.012	8.30 ± 0.29	32.9	1.11	0.374 ± 0.049 (47)
I1	35.0 ± 0.5	0.205 ± 0.013	5.00 ± 0.26	34.1	1.03	0.358 ± 0.078 (36)
I6	34.9 ± 0.5	0.551 ± 0.006	3.95 ± 0.06	16.0	2.18	0.349 ± 0.031 (45)
I12	39.2 ± 1.0	0.466 ± 0.046	4.81 ± 0.05	17.5	2.24	0.322 ± 0.023 (41)

[a] This set of steady-state ATPase values were determined contemporaneously on the same batch of MTs. A previous independence determination with wild-type DKH405 yielded 44 s^{-1} and 0.143 μM for k_{cat} and $K_{0.5(MT)}$, respectively (*11*). [b] Rate constant for bimolecular stimulation by MTs of mantADP release. Reactions were performed by mixing DKH405·mantADP plus carrier mantADP with MTs and ATP. Final concentrations were 0.1 and 1 μM for DKH405 and MTs, respectively, and 1 mM MgATP. PEP was also included at 2 mM to match the composition of the ATPase reaction. [c] Calculated as $(k_{cat}/K_{0.5(MT)})/k_{bi(ADP)}$. [d] Calculated as $(K_{0.5(MT)})(k_{bi(ADP)})$. [e] Sliding velocity of axonemes in multimotor mode as described in Materials and Methods. Reported as ±standard deviation (number of determinations).

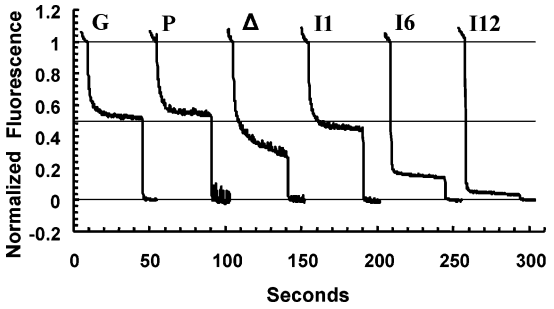

FIGURE 3: Release of mantADP from the tethered head. Reactions were performed by sequential additions to a stirred cuvette. Each trace was initiated by addition of a k405·mantADP complex to 0.25 μM, followed by addition of MTs to 1 μM after 6 s and MgATP to 200 μM after 42 s. The traces were normalized to 1 and 0 for the level of fluorescence before addition of MTs and after addition of ATP, respectively. Lines at normalized values of 0, 0.5, and 1 are included for reference. Fluorescence excitation was at 356 nm.

dimers (*26*). There are also modest changes in the $k_{bi(ADP)}$ for bimolecular stimulation of ADP release by MTs, with the Δ construct having an elevated rate and the I6 construct having a decreased rate.

Half-Site ADP Release. Release of ADP from dimeric DKH405 on binding to MTs is a two-step process, as indicated in Scheme 1, with the first ADP per dimer being released rapidly via k_{bi-MT} and the second ADP being released much more slowly in the absence of nucleotide via k'_o. Over a wide range of concentrations of free ADP, the predominant intermediate at equilibrium is the tethered species with one head tightly attached to the MT, without a bound ADP, and the other head containing a bound ADP (*15*, *27*). The results of Figure 3 indicate that the G, P, Δ, and I1 constructs are essentially identical to wild-type in this regard. Note that the experiments of Figure 3 were performed identically to that of Figure 1b of ref *15* to facilitate comparison to wild-type. This experiment uses the fluorescent ADP analogue, mantADP, whose fluorescence decreases on release from kinesin and has been a useful probe (*28*, *29*). DKH405, with two bound mantADP molecules, releases half its mantADP on addition of MTs, as indicated by the magnitude of the fluorescence decrease on mantADP dissociation for wild-type in Figure 3. The second mantADP remains bound until being chased off by excess ATP with completion of the full fluorescence decrease. The bound mantADP of the tethered intermediate of the Δ mutant construct is less stable, but similar to wild-type at a slightly lower free mantADP concentration (trace a of Figure 1 of ref *15*).

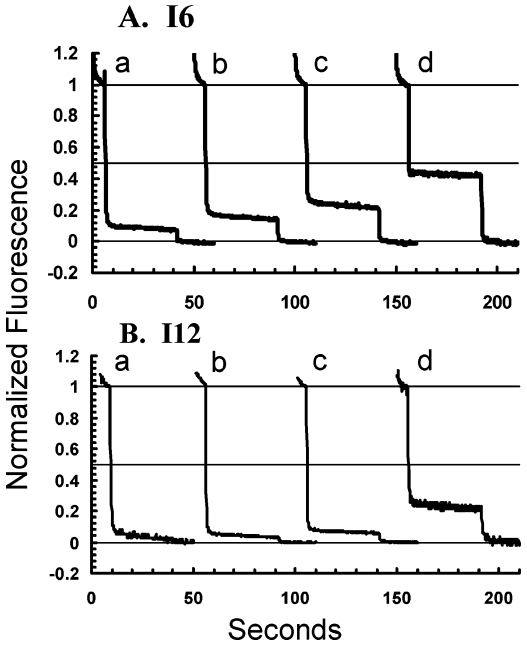

FIGURE 4: Dependence of time course of mantADP release from the tethered head on the level of free mantADP for the I6 and I12 constructs. Traces were obtained and normalized as in Figure 3, with addition of mantADP-DKH405 at 0.1 μM in trace a and at 0.25 μM in traces b−d. Free mantADP was included before addition of DKH405 at 0.25 and 3 μM for traces c and d, respectively. Trace b in each panel is from Figure 3. (A) DKH405-I6; (B) DKH405-I12.

The pattern for I6 and I12 in Figure 3 is very different. Significantly, more than half of the total fluorescence change occurs in the rapid phase on addition of MTs. Some mantADP remains bound, however, suggesting that the binding of mantADP to the tethered head is reversible under these conditions, but weaker. This is confirmed by the experiments of Figure 4, in which the amount of mantADP remaining bound to the tethered head at equilibrium increases with the concentration of free mantADP. Note that these experiments were also performed identically to the concentration series of Figure 1 of ref *15* to facilitate comparison to wild-type. The dependence of the amount of bound mantADP on the concentration of free mantADP (Figure 5) is consistent with a K_d of 0.43 μM for binding to the tethered head of the I6 construct. The corresponding value for the I12 construct is ∼5 μM, but is not well defined because binding is still only partial at 3 μM free mantADP.

Nucleotide-Independent Release of ADP from the Tethered Head. The rate of release of mantADP from the tethered

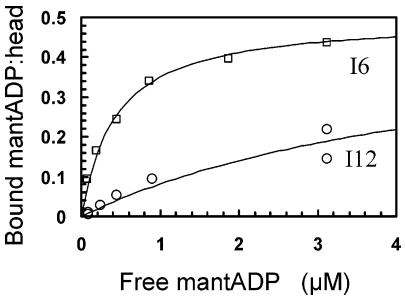

FIGURE 5: Dependence of level of mantADP bound to the tethered head on the free mantADP concentration for the I6 and I12 constructs. The normalized amount of mantADP remaining bound to the tethered head after addition of MTs was calculated from the traces in Figure 4 as the fraction released by ATP, relative to the total released in the ATP and MT dependent phases. Plot also contains results from other measurements not included in Figure 4. The level of free mantADP after addition of MTs was calculated from the amount of added carrier mantADP plus the amount of mantADP released on addition of MTs. The indicated lines were obtained by nonlinear regression for a binding equilibrium with a saturation value fixed at 0.5 mantADP:head. The K_d values obtained from the fit are 0.43 and 5.1 μM for the I6 and I12 constructs, respectively.

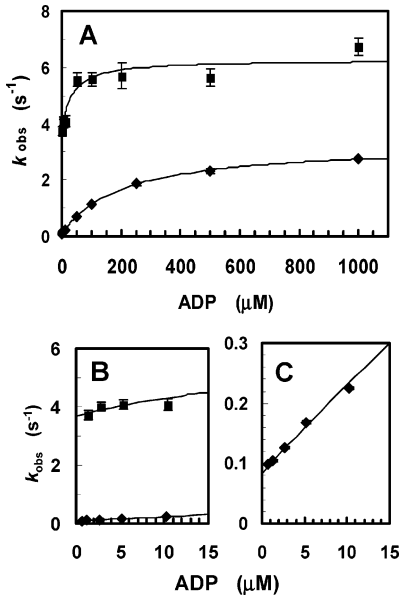

FIGURE 6: ADP-induced release of mantADP from the tethered head of the I1 (◆) and I6 (■) constructs. Reaction was performed by mixing buffer containing ADP as indicated with a tethered MT complex of DKH405. The complex was formed from 4 μM MTs, 0.8 μM DKH405·mantADP, and 0.2 μM carrier mantADP (all as 2× concentrations before mixing with the chase ADP). Under these conditions, kinesin will release at least half of its mantADP on binding to the MTs to generate ≥0.6 μM free mantADP. The results of Figures 3−5 indicate that this should produce a stable tethered complex with its tethered head largely saturated with mantADP for DKH405-I1, but saturation for DKH405-I6 is not complete.

head in the absence of nucleotide binding to the attached head, k'_o, can be determined as the limiting value of the ADP-induced release reaction on extrapolation to zero ADP (*15*). The dependence of the rate of mantADP release on the ADP concentration for I1 (Figure 6A) is essentially identical to that determined previously with wild-type (Figure 3 of ref *15*). The limiting value in the absence of free ADP (Figure 6C) defines k'_o for I1 as 0.08 s^{-1}, compared to 0.05 s^{-1} for wild-type (*15*). The rates with a chase of 1 μM ADP were also determined for the G, P, Δ, and I1 constructs as an approximation of k'_o in the absence of ADP. As indicated in Table 2, the nucleotide-independent rates for these constructs are also slow, at <0.16 s^{-1}, and similar to those for wild-type. With the I6 construct, however, the extrapolated rate in the absence of free ADP is much faster at 3.7 s^{-1} (Figure 6B), with an average value of 4 s^{-1} from a larger data set at 1 μM ADP (Table 2). This accelerated release of ADP from the tethered head with I6 is consistent with the weaker equilibrium binding of ADP to the tethered head of this construct, as observed above.

Table 2: Reactions of Tethered Intermediate

DKH405	$\sim k'_o$[a,b] (s^{-1})	$k_{t(T)}$[c,d] (s^{-1})	$k_{off(D)}$[c,e] (s^{-1})
wt	0.085 ± 0.001	255 ± 25 (11)	15.0 ± 2.1 (21)
G	0.110 ± 0.001	227 ± 23 (9)	15.7 ± 4.0 (8)
P	0.112 ± 0.001	245 ± 27 (14)	17.1 ± 5.2 (14)
Δ	0.153 ± 0.003	242 ± 45 (13)	17.1 ± 3.5 (12)
I1	0.119 ± 0.004	180 ±29 (12)	17.8 ± 4.1 (13)
I6	3.97 ± 0.18	172 ± 26 (7)	21.4 ± 6.3 (22)
I12	∼35	161 ± 38 (14)	22.0 ± 4.2 (24)

[a] ±standard error. [b] Estimated as the rate with a chase at 1 μM ADP. [c] ±standard deviation (number of determinations). [d] Obtained with pig MTs. [e] Determined by decrease in turbidity as previously described (*15*). Final concentration of KCl was 75 mM.

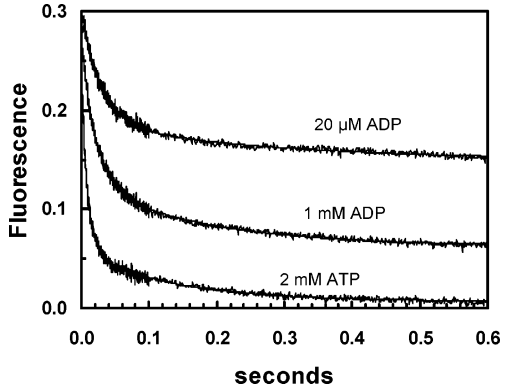

FIGURE 7: Nucleotide-induced release of mantADP from the tethered head of the I12 construct. Experiments were performed as in Figure 6, except that the weaker binding of mantADP by the tethered head of I12 required that the concentrations of MTs and DKH405-I12 be increased so that a reasonable fraction of the tethered heads had bound mantADP at the start of the reaction. The complex was formed with 16 μM MTs and 4 μM DKH405-I12 (before mixing with nucleotide). This results in 39% of the tethered heads having a bound mantADP, for a K_d of 5 μM (Figure 5). The transients are averages of 6−9 traces with final chase concentrations of 20 μM and 1 mM MgADP and 2 mM MgATP, as indicated. Curves were fit to a double-exponential decay, and the fit is indicated as a smooth line. The values from the fit were 34, 48, and 111 s^{-1}; 4, 6, and 8 s^{-1}; and 0.75, 0.68, and 0.78 for the rates of the fast and slow phases and the fraction of the total amplitude in the fast phase for 10 μM and 1 mM MgADP and 2 mM MgATP, respectively. The starting values of the transients have been offset for clarity.

Because of the weak binding of ADP by the tethered head of I12, it was necessary to increase the concentrations of MTs and DKH405-I12 so that a reasonable fraction of the tethered heads had bound mantADP at the start of the reaction. An averaged fluorescence transient for six traces at final concentrations of MTs, DKH405-I12, and chase ADP of 8, 2, and 20 μM is given in Figure 7. The transient was fit with a double exponential to yield a rate of 34 s^{-1} for the rapid phase with 75% of the total amplitude. A similar data set at 10 μM final chase ADP yielded a rate of 36 s^{-1}. Thus,

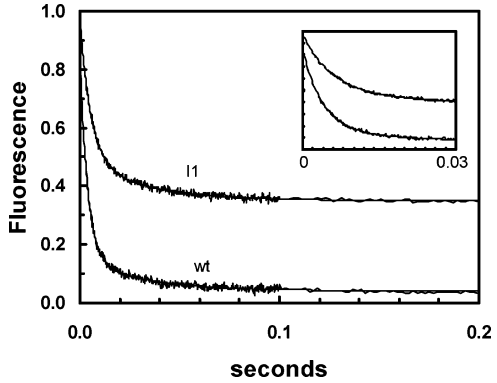

FIGURE 8: ATP-induced release of mantADP from the tethered head of wild-type and I1 constructs. Reactions were performed as in Figures 6 and 7, except that the complex was formed from 6 μM MTs and 1 μM DKH405 (2× concentrations before mixing with nucleotide). The final concentration of MgATP was 2 mM. The values from the fit were 254 and 177 s^{-1}; 32 and 31 s^{-1}; and 0.86 and 0.78 for the rates of the fast and slow phases and the fraction of the total amplitude in the fast phase for wild-type and I1, respectively.

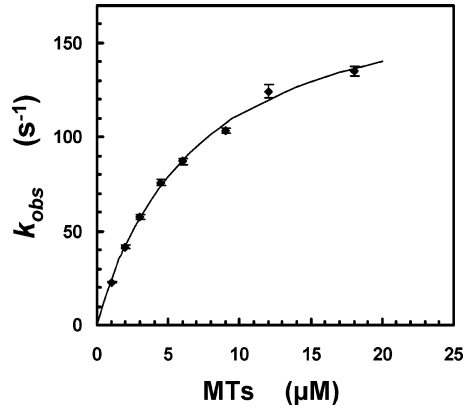

FIGURE 9: MT-induced ADP release from DKH365. A DKH365·mantADP complex was mixed with varying concentrations of MTs, and the rate of the fast phase of the fluorescent transient was determined. The final concentration of MgATP was 1 mM. The concentration of DKH365 was increased with increasing MTs, but the ratio of DKH365:MTs was always greater than 5:1. Nonlinear regression yielded values of 190 ±6 s^{-1} for k_{cat} and 7 ±0.5 μM for $K_{0.5}$.

a value of ~35 s^{-1} is a reasonable estimate of k'_o for DKH405-I12. Figure 7 also contains the averaged trace for reactions containing a saturating level of ADP in the chase. The rate for the fast phase of the averaged trace with 1 mM ADP is 48 s^{-1}, indicating little acceleration by high ADP concentrations.

ATP-Induced Release of ADP from the Tethered Head. ATP binding to the rigor head induces rapid ADP release from the tethered head, and this plays a critical role in reducing the probability of the dimer having two heads in the weak binding state simultaneously. The rates of ATP-induced mantADP release for a chase with an approximately saturating level of 2 mM ATP were determined, and representative averaged transients for I1 and wild-type are indicated in Figure 8. As discussed previously (*15*), the transient for wild-type is not a simple first-order process, and this is also true for DKH405-I1. When fitted to a double exponential, the fast phases had rates of 254 and 179 s^{-1} and amplitudes of 86% and 78% for wild-type and I1, respectively. The average rates determined from the individual traces are given in Table 2 for all the constructs.

ADP-Induced Dissociation of Kinesin from the MT. Binding of ADP to the rigor head of a tethered dimer produces a species that dissociates from the MT more rapidly because both heads have bound ADP and are in the weak binding state. This dissociation of the kinesin dimer from the MT can be monitored by turbidity (see ref *15*), and the dissociation rates for the mutant junction constructs are given in Table 2 at an approximately saturating concentration of ADP. This experiment was performed at a final KCl concentration of 75 mM to increase the extent of dissociation from the MT on addition of ADP. The dissociation rates of the I6 and I12 constructs are elevated with respect to the others, but not by a large factor.

MT-Induced ADP Release from Monomeric DKH365. The kinetics of MT-induced ADP release for monomeric DKH365 were determined (Figure 9) under approximately the same conditions used for determination of the nucleotide-stimulated release of ADP from the tethered intermediate. The extrapolated value at saturating levels of MTs is ~190 s^{-1}.

DISCUSSION

The neck linker plays a critical role in generation of motility, and previous mutations in this region have resulted in significant inhibition of ATPase and motility (*30*). Other studies have focused on the neck coil with disruptions or additions intended to stabilize or destabilize the coiled-coil in this region (*31*). Changes in the neck coil generally do not greatly disrupt motor domain function as monitored by the k_{cat} value, but they do influence processivity (*32*). Increased charge in the neck coil can even increase processivity (*32*), possibly due to increased interactions between the neck coil and the highly negatively charged C-terminal region of tubulin (E-hook). The constructs studied here involve changes at the junction of the neck linker and neck coil, and none of them exhibited significantly reduced values for either the k_{cat} or the rate of motility (Table 1), consistent with the lack of any change in the motor domain itself. The $k_{bi(ADP)}$ values for bimolecular binding of the dimer to MTs with release of ADP are also similar, although DKH405-Δ has a slightly elevated rate and the constructs with inserts are slightly slower than wild-type. The small decreases in $k_{bi(ADP)}$ and increases in $k_{off(D)}$ with the I6 and I12 constructs (Tables 1 and 2) may be due to decreased interaction of the neck coil with the tubulin E-hook caused by introduction of the long spacers.

The mutant junction constructs, however, do have significant differences in their extent of kinetic processivity. Both the Δ and I1 constructs have a modest decrease in the extent of kinetic processivity, as indicated by a <2-fold decrease in $k_{bi(ratio)}$ for the number of ATPs hydrolyzed per encounter and a 50−60% increase in the rate of dissociation from the MT during steady-state ATPase, $k_{off(ATPase)}$. The I6 and I12 constructs had much larger decreases in processivity, with over a 3-fold increase in their $k_{off(ATPase)}$ values compared to wild-type. Strikingly, the I6 and I12 constructs show greater than half-site ADP release on addition of MTs (Figure 3) and significantly weaker net binding of ADP to the tethered head (Figures 4 and 5). This weaker net binding of ADP results from a greatly accelerated rate of ADP release from the tethered head in the absence of nucleotide binding to the attached head (Figures 6 and 7 and Table 2). The rate of

35 s^{-1} for k'_o with I12 is a 700-fold increase over the value of 0.05 s^{-1} for the wild-type (*15*). Thus, the insertion of a spacer at the neck junction allows the tethered head to interact productively with the MT and release ADP rapidly. These results support the interpretation that the wild-type tethered intermediate cannot release ADP rapidly because the linkage between the two heads does not allow the tethered head to "reach" far enough to productively interact with a neighboring tubulin binding site. The added spacer allows the tethered head to reach farther and thus release ADP more rapidly.

The $k_{t(T)}$ value for wild-type of 255 s^{-1} with pig MTs (Table 2) is similar to that with bovine MTs (ref *15* and additional unpublished determinations) and also comparable to the maximum rate of ADP release from a monomer−MT complex of ~190 s^{-1} for DKH365 (Figure 9). Previous measurements of the maximum ADP release rate with monomers have yielded a wide range of values (see ref *15* for discussion). DKH365 has an advantage for determination of the maximum rate, in that it has a high $k_{bi(ADP)}$ rate of 27 μM^{-1} s^{-1}, even in the presence of 25 mM KCl. The similar values for the maximum rate of ADP release rate from the tethered wild-type and monomeric DKH365 suggest that there is no large special advantage gained by wild-type kinesin from possible steering of the tethered head to the correct MT site and the avoidance of unproductive interactions or increased disorder in the weak binding mode. The similar rates for maximum ADP release from a bound monomer and from the tethered head of a dimer on addition of ATP could also be a consequence of the tethered head of even the wild-type dimer being predocked on the MT, as in case C or D of Figure 2. The rates for the G, P, and Δ constructs are also of similar magnitude, and thus any disorder or incorrect orientation of these junction regions does not significantly decrease the rate at which the tethered head can find a MT binding site when ATP is present on the attached head.

The $k_{t(T)}$ values of the I1, I6, and I12 constructs are decreased from that of wild-type, and this may reflect increased disorder in the tethered complex formed by binding of ATP to the attached head. In the model put forth by Rice et al. (*9*), the docking of the neck linker of the attached head on binding of ATP would shift the tethered head into a position near the next tubulin binding site in the plus direction and would facilitate binding to that site with release of ADP. Introduction of a flexible spacer at the end of the neck linker would allow the tethered head to move away from this optimal position and would require a longer diffusional search before attachment at the correct site could occur. Although the inserts in I6 and I12 contain multiple glycine residues and should not be rigid, it is also possible that the $k_{t(T)}$ values are lower because the spacers have preferred conformations that direct the tethered head away from the proper tubulin binding site. The striking feature, however, is not that $k_{t(T)}$ is slightly less for the mutants, but rather that the values of $k_{t(T)}$ are so similar for I6 and I12 compared to the wild-type. One possibility is that the tethered head of species II (Scheme 1) for the mutants may more readily form a weak binding interaction with an adjoining MT binding site and be predocked on the MT before addition of ATP.

The rate of 4 s^{-1} for k'_o of I6 is fast, but still much slower than the rate of ADP release stimulated by binding of ATP to the attached head, $k_{t(T)}$, of 172 s^{-1}. Thus, I6 likely represents case C of Figure 2, in which the tethered head can attach to the MT with release of ADP, but the doubly attached dimer, without nucleotide at either head, is strained. The rate of 35 s^{-1} for k'_o of I12 is much faster, though, and indicates that I12 is more similar to case D, in which both heads can readily attach in the absence of nucleotide. I12 is not, however, completely converted to case D because the ATP-induced rate of 161 s^{-1} (Figure 7) is faster, and this indicates that even with this longer insert, binding of ATP to the attached head still facilitates attachment of the tethered head. Note that the 6 and 12 amino acid inserts in I6 and I12 are large on the scale of the kinesin dimer. The neck linker, indicated by the heavier line in Figure 1B, is also 12 amino acids long (from I^{325} to Thr^{336} in rat kinesin), and thus the two inserts of 12 residues in the I12 dimer would allow the heads to move apart by the length of the heavier line in Figure 1B. In fact, the two inserts in the I12 dimer, if extended, would themselves span the full 8-nm separation between tubulin binding sites along a protofilament. In this context, it is somewhat surprising that the insertion of 6 residues in I6 does not produce an even greater increase in k'_o than the 4 s^{-1} that is observed.

Analysis of wild-type DKH405 (*15*) indicated that a major route for dissociation of the dimer from the MT during steady-state ATPase is premature hydrolysis of ATP on the attached head before ADP can be released from the tethered head (conversion of IV to III in Scheme 1). Intermediate III can then dissociate via $k_{off(D)}$, although most of III will release ADP via $k_{t(D)}$, which is faster. A 37% decrease in $k_{t(T)}$ for I12 compared to wild-type and a 47% increase in $k_{off(D)}$ are in the correct direction for a decrease in processivity, but are too small to account for the full decrease. The remaining decrease in processivity could potentially be due to a number of causes. One possibility is a decreased rate of hydrolysis of ATP by the attached head, but this is unlikely because the k_{cat} is not significantly decreased. A more likely possibility is that ADP release from the tethered head is followed immediately by ATP binding to that head, without having to wait for the original attached head to hydrolyze its ATP. Concurrent hydrolysis on both heads would be more likely to produce species III, with ADP at both heads, and thus result in more rapid net dissociation from the MT. Such inhibition of ATP binding to V is a natural consequence of the Rice et al. model (*9*) because the two heads of the dimer cannot be both attached and have docked neck linkers, without substantial unwinding of the neck coil. Rosenfeld et al. (*33*) recently reported evidence for such inhibition of ATP binding to the empty head of a dimer bound to a MT with one attached head containing bound AMP−PNP. Addition of a long insert, as in I6 and I12, would largely remove any steric basis for this inhibition of ATP binding to species V.

Because an increased rate for k'_o should favor formation of the tightly bound species X′ for I6 and I12, it may at first appear paradoxical that net binding to MTs during ATP hydrolysis is actually weaker for the constructs with long junction inserts ($K_{0.5(MT)}$ values of ~0.5 μM versus 0.12 μM for wild-type). Although the more rapid rate of formation of X′ with a second rigor head would, in fact, produce tighter net binding in the absence of nucleotide or in the presence of low ADP for I6 and I12, it would not significantly increase processivity in the presence of high ATP, because ATP

binding to the attached head via k_{bi-T} at ~700 s^{-1} (*34*) is so much faster than k'_o at 35 s^{-1} for I12. Thus, in the presence of saturating levels of ATP, species II will usually partition to species IV and then V, rather than to X′, even for the I12 construct. Net dissociation during ATP hydrolysis is principally controlled by the fraction of the steady-state population that is present as the weakly bound species III. The breakdown in coordination of the ATPase cycles of the two heads for I6 and I12 will increase the fraction as species III at steady state and thus increase the rate of dissociation and decrease the extent of kinetic processivity. It might also be expected that the rate of ADP-stimulated dissociation of the dimer from the MT ($k_{off(D)}$) would be slower with the I6 and I12 mutants with both heads attached than from the wild-type, when in fact it is slightly faster (22 s^{-1} for I12 versus 15 s^{-1} for wild-type). One possibility is that the tethered head of the wild-type dimer is also weakly bound to the MT, and thus the complexes of I12 and the wild-type with two bound ADP molecules do not differ greatly. There may also be less interaction between the neck coil of I12 and the E-hook, as discussed above.

The observed extent of kinetic processivity with I6 and I12 may represent the limiting processivity for two physically linked, but kinetically uncorrelated monomer heads. If net dissociation at 2.2 s^{-1} for $k_{off(ATPase)}$ is principally via $k_{off(D)}$ at 22 s^{-1}, then species III must be 10% of the steady-state population. For uncorrelated heads, this would correspond to each head being in the ADP or weak binding state for ~32% of its ATPase cycle. Monomer head domains themselves hydrolyze ATP processively (*35*, *36*), and 32% is a reasonable estimate for the fraction in a weak binding state. For example, the maximum ADP release rate of ~200 s^{-1} from the MT·E·ADP complex of the monomer DKH365 (Figure 9) requires that the total rate limitation in the rest of the cycle is only ~90 s^{-1}, to yield the observed k_{cat} value of ~61 s^{-1} for DKH365 and other full-length monomers (*11*). This results in an estimated ~31% of the MT·DKH365 complex being present as the ADP species during steady-state hydrolysis at saturating levels of MTs.

The work presented here shows that the two head domains of the I6 and I12 constructs have lost most, but not all, of the coordination of their ATPase cycles with a decrease in kinetic processivity. An interesting issue for future work is whether this decrease in kinetic processivity results in a decrease in processivity of movement along the MT.

ACKNOWLEDGMENT

We thank Mark Bier of the Center for Molecular Analysis (NSF instrument grant CHE-9808188) for mass spectral measurements; Gregory Fisher, Gregory Larocca, and Fredrick Lanni for advice on DIC microscopy and the Center for Light Microscope Imaging and Biotechnology (NSF STC grant MCB-8920118) for access to microscopy facilities; Lee Ziegler and Christopher Eggers for assistance in cloning; Jing-Qui Cheng and Wei Jiang for participation in early stages of the work; and Heidi Browning for critical reading of the manuscript.

REFERENCES

1. Vale, R. D., and Milligan, R. A. (2000) *Science 288*, 88−95.
2. Goldstein, L. S., and Philp, A. V. (1999) *Annu. Rev. Cell Dev. Biol. 15*, 141−183.
3. Sack, S., Kull, F. J., and Mandelkow, E. (1999) *Eur. J. Biochem. 262*, 1−11.
4. Howard, J., Hudspeth, A. J., and Vale, R. D. (1989) *Nature 342*, 154−158.
5. Block, S. M., Goldstein, L. S., and Schnapp, B. J. (1990) *Nature 348*, 348−352.
6. Hackney, D. D. (1996) *Annu. Rev. Physiol. 58*, 731−750.
7. Hackney, D. D. (1988) *Proc. Natl. Acad. Sci. U.S.A. 85*, 6314−6318.
8. Hackney, D. D. (1994) *Proc. Natl. Acad. Sci. U.S.A. 91*, 6865−6869.
9. Rice, S., Lin, A. W., Safer, D., Hart, C. L., Naber, N., Carragher, B. O., Cain, S. M., Pechatnikova, E., Wilson-Kubalek, E. M., Whittaker, M., Pate, E., Cooke, R., Taylor, E. W., Milligan, R. A., and Vale, R. D. (1999) *Nature 402*, 778−784.
10. Yang, J. T., Saxton, W. M., and Goldstein, L. S. (1988) *Proc. Natl. Acad. Sci. U.S.A. 85*, 1864−1868.
11. Jiang, W., Stock, M., Li, X., and Hackney, D. D. (1997) *J. Biol. Chem. 272*, 7626−7632.
12. Stock, M. F., Guerrero, J., Cobb, B., Eggers, C. T., Huang, T.-G., Li, X., and Hackney, D. D. (1999) *J. Biol. Chem. 274*, 14617−14623.
13. Itakura, S., Yamakawa, H., Toyoshima, Y. Y., Ishijima, A., Kojima, T., Harada, Y., Yanagida, T., Wakabayashi, T., and Sutoh, K. (1993) *Biochem. Biophys. Res. Commun. 196*, 1504−1510.
14. Stock, M. F., and Hackney, D. D. (2001) in *Methods in Molecular Biology—Kinesin Protocols* (Vernos, I., Ed.) pp 43−48, Humana Press, Totawa, NJ.
15. Hackney, D. D. (2002) *Biochemistry 41*, 4437−4446.
16. Huang, T. G., and Hackney, D. D. (1994) *J. Biol. Chem. 269*, 16493−16501.
17. Stock, M. F., and Hackney, D. D. (2001) in *Methods in Molecular Biology—Kinesin Protocols* (Vernos, I., Ed.) pp 65−71, Humana Press, Totawa, NJ.
18. Huang, T.-G., and Hackney, D. D. (1994) *J. Biol. Chem. 269*, 16493−16501.
19. Hackney, D. D., Levitt, J. D., and Wagner, D. D. (1991) *Biochem. Biophys. Res. Commun. 174*, 810−815.
20. Kozielski, F., Sack, S., Marx, A., Thormahlen, M., Schonbrunn, E., Biou, V., Thompson, A., Mandelkow, E. M., and Mandelkow, E. (1997) *Cell 91*, 985−994.
21. Hoenger, A., Thormahlen, M., Diaz-Avalos, R., Doerhoefer, M., Goldie, K. N., Muller, J., and Mandelkow, E. (2000) *J. Mol. Biol. 297*, 1087−1103.
22. Hackney, D. D., and Clark, P. K. (1984) *Proc. Natl. Acad. Sci. U.S.A. 81*, 5345−5349.
23. Conibear, P. B., and Geeves, M. A. (1998) *Biophys. J. 75*, 926−937.
24. Cremo, C. R., and Geeves, M. A. (1998) *Biochemistry 37*, 1969−1978.
25. Walker, M. L., Burgess, S. A., Sellers, J. R., Wang, F., Hammer, J. A., III, Trinick, J., and Knight, P. J. (2000) *Nature 405*, 804−807.
26. Hackney, D. D. (1994) *J. Biol. Chem. 269*, 16508−16511.
27. Hackney, D. D. (1994) *Proc. Natl. Acad. Sci. U.S.A. 91*, 6865−6869.
28. Sadhu, A., and Taylor, E. W. (1992) *J. Biol. Chem. 267*, 11352−11359.
29. Cheng, J. Q., Jiang, W., and Hackney, D. D. (1998) *Biochemistry 37*, 5288−5295.
30. Case, R. B., Rice, S., Hart, C. L., Ly, B., and Vale, R. D. (2000) *Curr. Biol. 10*, 157−160.
31. Romberg, L., Pierce, D. W., and Vale, R. D. (1998) *J. Cell Biol. 140*, 1407−1416.
32. Thorn, K. S., Ubersax, J. A., and Vale, R. D. (2000) *J. Cell Biol. 151*, 1093−1100.
33. Rosenfeld, S. S., Fordyce, P. M., Jeffereson, G. M., King, P. H., and Block, S. M. (2003) *J. Biol. Chem. 278*, 18550−18556.
34. Rosenfeld, S. S., Xing, J., Jefferson, G. M., Cheung, H. C., and King, P. H. (2002) *J. Biol. Chem. 277*, 36731−36739.
35. Jiang, W., and Hackney, D. D. (1997) *J. Biol. Chem. 272*, 5616−5621.
36. Ma, Y. Z., and Taylor, E. W. (1997) *J. Biol. Chem. 272*, 717−723.
37. Sayle, R., and Milner-White, E. J. (1995) *Trends Biochem. Sci. 20*, 374.

BI0349118